
Quantitative SPECT/CT Metrics in Early Prediction of [¹⁷⁷Lu]Lu-DOTATATE Treatment Response in Gastroenteropancreatic Neuroendocrine Tumor Patients

Onur Tuncer¹, Daniel Steinberger², Joseph Steiner³, Madeleine Hinojos⁴, Stephanie Y. Rhee⁵, Brad Humphrey⁶, Farhad Jafari⁷, and Zuzan Cayci²

¹Department of Radiology, University of Minnesota Medical School, Minneapolis, Minnesota; ²Nuclear Medicine Division, Department of Radiology, University of Minnesota Medical School, Minneapolis, Minnesota; ³Imaging Physics Division, Department of Radiology, University of Chicago, Chicago, Illinois; ⁴Department of Radiology, Oregon Health and Science University School of Medicine, Portland, Oregon; ⁵University of Minnesota Medical School, Minneapolis, Minnesota; ⁶Radiotheranostics Unit, M Health Fairview University of Minnesota Medical Center, Minneapolis, Minnesota; and ⁷Medical Physics Division, Department of Radiology, University of Minnesota Medical School, Minneapolis, Minnesota

Our objective is to explore quantitative imaging markers for early prediction of treatment response in patients with gastroenteropancreatic neuroendocrine tumors (GEP-NETs) undergoing [¹⁷⁷Lu]Lu-DOTATATE therapy. By doing so, we aim to enable timely switching to more effective therapies in order to prevent time-resource waste and minimize toxicities. **Methods:** Patients diagnosed with unresectable or metastatic, progressive, well-differentiated, receptor-positive GEP-NETs who received 4 sessions of [¹⁷⁷Lu]Lu-DOTATATE were retrospectively selected. Using SPECT/CT images taken at the end of treatment sessions, we counted all visible tumors and measured their largest diameters to calculate the tumor burden score (TBS). Up to 4 target lesions were selected and semiautomatically segmented. Target lesion peak counts and spleen peak counts were measured, and normalized peak counts were calculated. Changes in TBS (Δ TBS) and changes in normalized peak count (Δ nPC) throughout treatment sessions in relation to the first treatment session were calculated. Treatment responses were evaluated using third-month CT and were binarized as progressive disease (PD) or non-PD. **Results:** Twenty-seven patients were included (7 PD, 20 non-PD). Significant differences were observed in Δ TBS_{second-first}, Δ TBS_{third-first}, and Δ TBS_{fourth-first} (where second-first, third-first, and fourth-first denote scan number between the second and first, third and first, and fourth and first [¹⁷⁷Lu]Lu-DOTATATE treatment cycles), respectively) between the PD and non-PD groups (median, 0.043 vs. -0.049, 0.08 vs. -0.116, and 0.109 vs. -0.123 [$P = 0.023$, $P = 0.002$, and $P < 0.001$], respectively). Δ nPC_{second-first} showed significant group differences (mean, -0.107 vs. -0.282; $P = 0.033$); Δ nPC_{third-first} and Δ nPC_{fourth-first} did not reach statistical significance (mean, -0.122 vs. -0.312 and -0.183 vs. -0.405 [$P = 0.117$ and 0.067], respectively). At the optimal threshold, Δ TBS_{fourth-first} exhibited an area under the curve (AUC) of 0.957, achieving 100% sensitivity and 80% specificity. Δ TBS_{second-first} and Δ TBS_{third-first} reached AUCs of 0.793 and 0.893, sensitivities of 71.4%, and specificities of 85% and 95%, respectively. Δ nPC_{second-first}, Δ nPC_{third-first}, and Δ nPC_{fourth-first} showed AUCs of 0.764, 0.693, and 0.679; sensitivities of 71.4%, 71.4%, and 100%; and specificities of 75%, 70%, and 35%, respectively. **Conclusion:** Δ TBS and Δ nPC can predict [¹⁷⁷Lu]Lu-DOTATATE response by the second treatment session.

Key Words: Lutathera; [¹⁷⁷Lu]Lu-DOTATATE; GEP-NETs; treatment response; tumor burden score; SPECT/CT

J Nucl Med 2024; 65:1584-1590
DOI: 10.2967/jnumed.124.267964

In 2018, the Food and Drug Administration approved a peptide receptor radionuclide therapy, Lutathera (Novartis), for gastroenteropancreatic neuroendocrine tumors (GEP-NETs) for the first time (1). This innovative drug combines radionuclide ¹⁷⁷Lu with a somatostatin analog, (Tyr³)-octreotate (TATE), using DOTA as a chelator, resulting in the formation of a radiolabeled final product, [¹⁷⁷Lu]Lu-DOTATATE. The DOTATATE component of this compound acts as a decoy, binding to somatostatin peptide receptors, which are notably upregulated on the surface of neuroendocrine neoplastic cells (2). This binding triggers a receptor-mediated endocytosis; within the cell, emitted β -particles from the decay of ¹⁷⁷Lu result in DNA damage in the form of single- and double-strand breaks. The ultimate outcome is the selective eradication of neoplastic cells with minimal systemic toxicity (3).

The study that paved the way for Food and Drug Administration approval was the NETTER-1 trial (4), in which adults with inoperable, well-differentiated, metastatic midgut neuroendocrine tumors who had exhibited disease progression over the past 3 y while on octreotide were randomly assigned to either a [¹⁷⁷Lu]Lu-DOTATATE group (with long-acting 30-mg octreotide for symptom control) or a control group (long-acting 60-mg octreotide). The results unveiled a significant improvement in progression-free survival ($P < 0.001$) and objective response rate ($P < 0.001$) in the [¹⁷⁷Lu]Lu-DOTATATE group. In the interim analysis, overall survival was also statistically significant ($P = 0.004$), but in the final report, [¹⁷⁷Lu]Lu-DOTATATE treatment did not significantly improve median overall survival versus the control group (5). Nevertheless, there was an 11.7-mo difference in median overall survival between the 2 groups. These findings led to the approval and clinical application of [¹⁷⁷Lu]Lu-DOTATATE with an indication for progressive, unresectable, and well-differentiated (grade 1 or 2) GEP-NETs exhibiting positive somatostatin receptors. Furthermore, results from the NETTER-2 trial (NCT03972488) investigating outcomes for grade

Received Apr. 16, 2024; revision accepted Aug. 2, 2024.
For correspondence or reprints, contact Zuzan Cayci (cayci001@umn.edu).
Published online Sep. 12, 2024.
COPYRIGHT © 2024 by the Society of Nuclear Medicine and Molecular Imaging.

3 GEP-NETs are forthcoming. With the emerging preliminary analysis reports, studies suggest the broadening of the therapeutic scope of [¹⁷⁷Lu]Lu-DOTATATE beyond its initially defined indications, even suggesting its use as first-line therapy in the near future (6,7).

The current standard therapy consists of 4 infusions of 7.4 GBq of [¹⁷⁷Lu]Lu-DOTATATE every 2 mo, following the same schedule for every patient. However, given the highly heterogeneous nature of these neoplasms, the inherent variability among patients, the variations in disease burden along with future potential broadened indications, and the considerable cost associated with each treatment session, it becomes imperative to pursue a more precise patient selection process and a more personalized application approach early in the treatment. Specifically, determining patients who will not benefit from this treatment is important to avoid an additional delay of up to 8 mo in transitioning to a more suitable treatment strategy, such as transarterial radioembolization, as well as to prevent toxicities, resource waste, and unmet expectations. Our goal is to investigate quantitative imaging markers that can facilitate early prediction of treatment response to identify patients who do not respond to the treatment and to provide data for further elaboration of patient-specific dose and schedule adjustments for future clinical applications.

MATERIALS AND METHODS

Patient Selection

The institutional review board of the University of Minnesota approved this retrospective study (STUDY00014256-25, October 2021), and the requirement to obtain informed consent was waived. We conducted a retrospective review of our archives for patients diagnosed with unresectable or metastatic, progressive, well-differentiated, somatostatin receptor–positive GEP-NETs. The inclusion and exclusion criteria for our study are detailed in Figure 1. Demographic and clinical information, including age, sex, tumor locations, and pathology reports, as well as follow-up durations and clinical courses, were collected from the archives.

[¹⁷⁷Lu]Lu-DOTATATE Application

Treatment decisions were collaboratively determined according to an imaging assessment with [⁶⁸Ga]Ga-DOTATATE PET. All patients received 4 infusions of 7.4 GBq of [¹⁷⁷Lu]Lu-DOTATATE every

2 mo, injected from a single-dose vial containing 370 MBq/mL according to Food and Drug Administration guidelines (8). SPECT/CT images were taken 30 min after the end of the amino acid infusion, which corresponds to approximately 3.5 h after the completion of the [¹⁷⁷Lu]Lu-DOTATATE infusion, as per the standard protocol at our institution. A long-acting octreotide, 30 mg intramuscularly, was administered between 4 and 24 h after each dose and also every 4 wk after the completion of [¹⁷⁷Lu]Lu-DOTATATE treatment until disease progression or up to 18 mo after treatment initiation. All patients were administered an amino acid solution beginning 30 min before the [¹⁷⁷Lu]Lu-DOTATATE administration to mitigate the radiation dose to the kidneys.

Image Acquisition

SPECT/CT of the body part with the highest tumor load was performed 30 min after each treatment using a Symbia Intevo (Siemens) dual-head scanner equipped with 3/8-in NaI(Tl) scintillation crystals and medium-energy, parallel-hole collimators, using a single 15% energy window centered at a photo-peak energy of 208 keV. Low-dose CT images were acquired for attenuation correction and anatomic localization. The body part with the highest tumor load was determined by pretreatment [⁶⁸Ga]Ga-DOTATATE PET/CT. Third-month follow-up contrast-enhanced CT scans of the chest, abdomen, and pelvis were acquired with a 3-mm slice thickness.

Target Lesion Segmentation and Quantitative Metrics

For each patient, up to 4 target lesions were selected for segmentation on SPECT/CT performed after each treatment session under the supervision of an experienced nuclear medicine physician according to revised RECIST (9). Each target lesion was semiautomatically segmented with the commercially available Syngo.Via (Siemens Healthineers) software (10). Segmentation was done using the 40% threshold method, where voxels containing at least 40% of the maximum counts of the targeted lesion in the SPECT were selected (Fig. 2). Signal peak count, which is analogous to SUV_{peak} in PET (the maximum average value within a spheric 1 cm³ volume), was measured within each segmented target lesion and spleen.

Quantitative parameters included normalized peak count (nPC), nPC change (ΔnPC), tumor burden score (TBS), and TBS change (ΔTBS). These were calculated at the end of each treatment session.

TBS

First described by Sasaki et al. as a prognostic tool for colorectal cancer liver metastasis, TBS was shown in multiple studies to be an effective indicator of prognosis (11–14). All visible tumoral foci were counted, including all anatomic localizations, and their largest diameters were manually measured on axial CT images. The largest diameter of the largest tumor was used for TBS calculation. TBS and

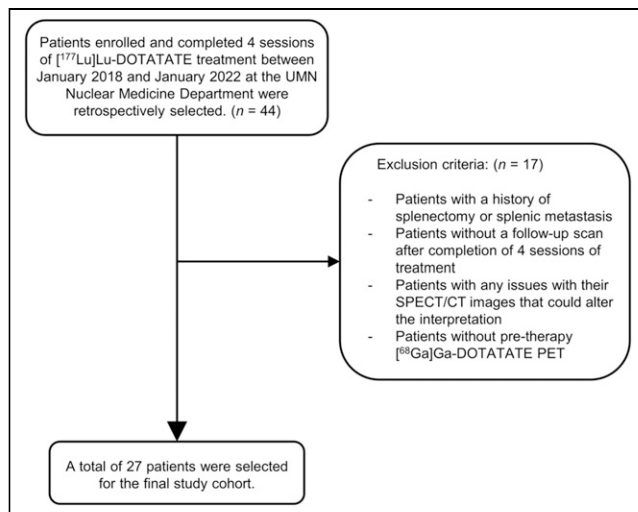


FIGURE 1. Patient selection flowchart. UMN = University of Minnesota.

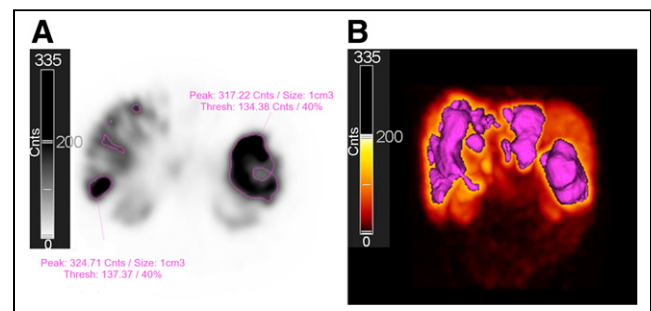


FIGURE 2. Target lesion segmentation with Syngo.Via software. (A) Segmented target lesions from posttreatment SPECT imaging. (B) Maximum-intensity projection showing 3-dimensional segmented target lesions from posttreatment images. Cnts = counts; Thresh = threshold.

TABLE 1
Demographic, Clinical, and Radiologic Characteristics of Response Groups

Variable	PD (n = 7)	Non-PD (n = 20)	P
Numeric			
Age (y)	68.29 (SD, 11.07)	63.35 (SD, 8.87)	0.245
Follow-up CT acquisition time (d)	73.43 (SD, 17.84)	72.26 (SD, 23.07)	0.905
Pretreatment maximum tumor diameter (cm)	7.1 (IQR, 4.2–11.2)	6.7 (IQR, 4.25–10.83)	0.868
Number of pretreatment tumor foci	4 (IQR, 3–11)	10 (IQR, 5.5–18)	0.052
TBS			
First scan	11.77 (IQR, 6.62–12.56)	13.23 (IQR, 10.27–19.8)	0.184
Second scan	11.44 (IQR, 9.27–14.53)	12.73 (IQR, 9.76–19.5)	0.507
Third scan	13.15 (IQR, 10.7–15.06)	10.6 (IQR, 7.93–17.15)	0.74
Fourth scan	13.8 (IQR, 11.45–15.58)	10.66 (IQR, 8.12–17.73)	0.825
Average peak count			
First scan	204.87 (IQR, 87.28–683)	531.79 (IQR, 319.57–934.27)	0.068
Second scan	211.28 (IQR, 102.93–494)	319.98 (IQR, 242.12–571.52)	0.293
Third scan	209.5 (IQR, 89.02–390.67)	307.3 (IQR, 190.28–419.75)	0.439
Fourth scan	165.5 (IQR, 113.75–327.15)	285.38 (IQR, 157.26–370.37)	0.293
nPC			
First scan	2.71 (SD, 1.98)	4.08 (SD, 1.98)	0.130
Second scan	2.24 (SD, 1.58)	2.84 (SD, 1.22)	0.307
Third scan	2.24 (SD, 1.64)	2.72 (SD, 1.56)	0.498
Fourth scan	2.2 (SD, 1.72)	2.28 (SD, 1.28)	0.9
Categoric			
Male sex	2/7 (28.6%)	8/20 (40%)	0.678
Ki-67 index			
<3	1/7 (14.3%)	3/19 (15.8%)	
3–20	4/7 (57.1%)	14/19 (73.7%)	
>20	2/7 (28.6%)	2/19 (10.5%)	0.566
Previous treatments			
SSA only	0/7 (0%)	4/20 (20%)	
SSA+ chemotherapy	3/7 (42.9%)	9/20 (45%)	
SSA + chemotherapy + TARE	0/7 (0%)	1/20 (5%)	
SSA+ surgery	2/7 (28.6%)	6/20 (30%)	
SSA + TARE	1/7 (14.3%)	0/20 (0%)	
Surgery + radiotherapy	1/7 (14.3%)	0/20 (0%)	0.223
Metastasis location			
Liver	7/7 (100%)	20/20 (100%)	
Gastrointestinal	4/7 (57.1%)	11/20 (55%)	1
Pancreas	2/7 (28.6%)	8/20 (40%)	0.678
Above diaphragm	3/7 (42.9%)	6/20 (30%)	0.653
Bone	3/7 (42.9%)	3/20 (15%)	0.290
Patient comments			
Better or stable at third month	5/7 (71.4%)	20/20 (100%)	0.06
Better or stable at sixth month	3/3 (100%)	16/17 (94.1%)	1

IQR = interquartile range (25–75); SSA = somatostatin analog; TARE = transarterial radioembolization.

Categoric data are number and percentage; numeric data are means with SDs or medians with interquartile ranges (25–75) according to normality distribution. P values were determined using Mann–Whitney U test or independent-samples t test for numeric variables or Fischer exact test for categoric variables.

Δ TBS were calculated using the following formula:

$$TBS^2 = (\text{number of all visible tumors})^2 + (\text{maximum tumor diameter})^2$$

$$\Delta TBS_{\text{scan number}-1\text{st scan}} = \frac{TBS \text{ at scan number} - TBS \text{ at first scan}}{TBS \text{ at first scan}}$$

nPCs

Average peak counts of target lesions after each scan were calculated and divided by spleen peak counts at the same scan, aiming to eliminate differences based on patient pharmacodynamics and injection time–image time interval between scans. The calculation of nPC and Δ nPC is as follows:

$$nPC = \frac{\text{average PC of target lesions}}{\text{spleen PC at the same scan}}$$

Similarly to Δ TBS, Δ nPC was calculated as follows:

$$\Delta nPC_{\text{scan number}-1\text{st scan}} = \frac{nPC \text{ at scan number} - nPC \text{ at first scan}}{nPC \text{ at first scan}}$$

Response Evaluation

Radiographic responses were assessed through third-month follow-up CT scans by an experienced nuclear medicine physician according to revised RECIST (9). Treatment responses were binarized as progressive disease (PD) or non-PD. Clinical responses at third-month and sixth-month routine oncology visits were noted from chart reviews and categorized as worse or as stable/better on the basis of the patients' own verbal comments regarding their symptoms.

Statistical Analysis

Descriptive statistics were calculated. The Shapiro–Wilk test was applied to assess for a normal distribution. The Mann–Whitney *U* test or independent-samples *t* test were used for comparison of numeric variables accordingly to normality distribution. The Fisher exact test was used for categorical variables. Statistical significance was set at a 2-tailed *P* value of less than 0.05. All statistical analyses were conducted using SPSS version 29 (IBM) and Prism version 10 (GraphPad Software).

TBS, Δ TBS, nPC, and Δ nPC values at each scan were compared with the treatment response. Receiver operating characteristic curves were drawn for Δ nTBS and Δ nPC; optimal cutoffs were determined according to the Youden index.

RESULTS

The final study cohort comprised 27 patients with 7 PD and 20 non-PD (Fig. 1). Between the PD and non-PD groups, there were no statistical differences in age, follow-up CT acquisition timing after therapy, pretreatment maximum tumor diameter and number of tumor foci, sex, or metastasis locations. Furthermore TBS, target lesion peak counts, and nPC at each respective scan did not show statistically significant differences between the 2 groups (Table 1). However, both TBS and nPC across 4 [¹⁷⁷Lu]Lu-DOTATATE treatment sessions demonstrated substantially different trends between the 2 groups (Figs. 3A and 3B).

TBS

In the PD group, the mean TBS values were 10.36 (\pm 3.6) at the first scan, 11.68 (\pm 3.16) at the second, 12.61 (\pm 3.13) at the third, and 12.81 (\pm 2.96) at the fourth. Initially lower than in the non-PD group, these values continued to increase despite the therapy. Conversely, the non-PD group exhibited a decreasing trend after the therapy initiation, with mean values of 14.2 (\pm 5.64) at the first scan, 13.6 (\pm 5.87) at the second, 12.47 (\pm 5.63) at the third, and 12.27

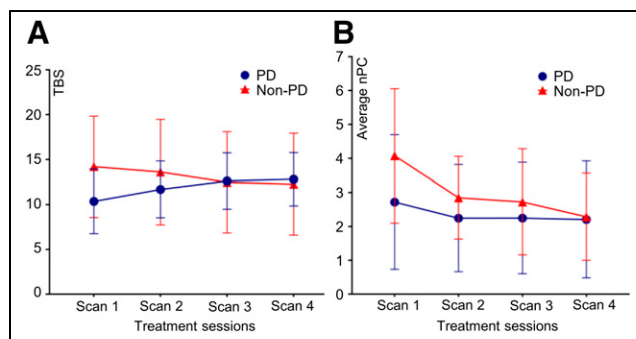


FIGURE 3. Mean TBS (A) and nPC (B) across 4 treatment sessions. Lines indicate SD.

(\pm 5.67) at the fourth. The most notable mean TBS decrease occurred during the third scan, falling below the PD group (Fig. 3A).

Δ TBS_{second-first}, Δ TBS_{third-first}, and Δ TBS_{fourth-first} (where second-first, third-first, and fourth-first denote the [¹⁷⁷Lu]Lu-DOTATATE treatment cycles (sessions) between posttreatment SPECT/CT obtained after cycle 2 and cycle 1, cycle 3 and cycle 1, and cycle 4 and cycle 1, respectively) all exhibited significant differences between the PD and non-PD groups (median values, 0.043 vs. -0.049 , 0.08 vs. -0.116 , and 0.109 vs. -0.123 [*P* = 0.023, *P* = 0.002, and *P* < 0.001], respectively). Significant differences started as early as at Δ TBS_{second-first}, which is an outcome of the first treatment session. Differences between the 2 groups became more prominent with the continuation of the therapy (Fig. 4; Table 2).

In the receiver operating characteristic curves, Δ TBS_{fourth-first} exhibited the best performance, with an area under the curve (AUC) of 0.957, achieving 100% sensitivity and 80% specificity. Δ TBS_{second-first} and Δ TBS_{third-first} reached AUCs of 0.793 and

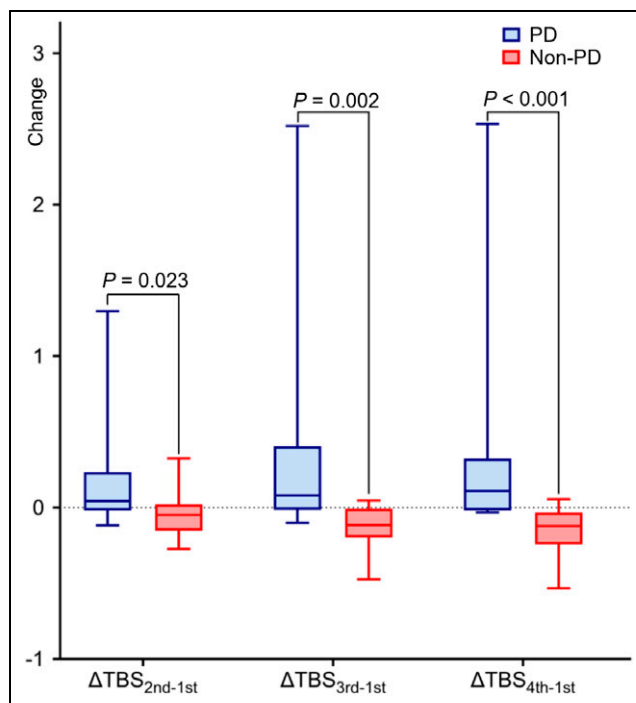


FIGURE 4. Box plots showing Δ TBS difference between PD and non-PD throughout treatment sessions. *P* values were calculated using Mann–Whitney *U* test.

TABLE 2
 Δ TBS and Δ PC Differences Between Response Groups

Parameter	PD		Non-PD		<i>P</i> [†]
	Median or mean*	95% CI	Median or mean*	95% CI	
Δ TBS _{second-first}	0.043	-0.019 to 1.296	-0.049	-0.135 to 0	0.023
Δ TBS _{third-first}	0.08	-0.015 to 2.519	-0.116	-0.194 to -0.028	0.002
Δ TBS _{fourth-first}	0.109	-0.018 to 2.533	-0.123	-0.197 to -0.035	<0.001
Δ PC _{second-first}	-0.107	-0.273 to 0.06	-0.282	-0.364 to -0.200	0.033
Δ PC _{third-first}	-0.122	-0.313 to 0.068	-0.312	-0.444 to -0.180	0.117
Δ PC _{fourth-first}	-0.183	-0.383 to 0.016	-0.405	-0.535 to -0.276	0.067

*Median reported for Δ TBS, and mean reported for Δ PC.
[†]*P* values were determined using Mann-Whitney *U* test or independent-samples *t* test for numeric variables.

0.893, sensitivities of 71.4%, and specificities of 85% and 95%, respectively (Table 3).

nPCs

The mean nPC values of the PD and non-PD groups were 2.71 (± 1.98) versus 4.08 (± 1.98) at the first scan, 2.24 (± 1.58) versus 2.84 (± 1.22) at the second, 2.24 (± 1.64) versus 2.72 (± 1.56) at the third, and 2.20 (± 1.72) versus 2.28 (± 1.28) at the fourth. The mean nPC between the 2 groups did not exhibit statistically significant differences at any scans. However, the PD group displayed a stable trend, whereas the non-PD group showed a decreasing trend, which was the most prominent from the first to the second scans (Fig. 3B). The mean nPC was higher at the beginning of therapy in the non-PD group; by the end of fourth scan, it was nearly equal to the PD group.

When Δ nPC values were investigated, Δ nPC_{second-first} showed statistically significant differences between the PD and non-PD groups (mean, -0.107 vs. -0.282; *P* = 0.033), whereas Δ nPC_{third-first} and Δ nPC_{fourth-first} did not significantly differ between groups (mean, -0.122 vs. -0.312 and -0.183 vs. -0.405 [*P* = 0.117 and 0.067], respectively; Table 2; Fig. 5).

The receiver operating characteristic curves of Δ nPC reached the highest AUC, 0.764, at Δ nPC_{second-first}, with sensitivity of 71.4% and specificity of 75% at the optimal threshold. Δ nPC_{third-first} and Δ nPC_{fourth-first} reached AUCs of 0.693 and 0.679, sensitivities of 71.4% and 100%, and specificities of 70% and 35%, respectively, at the optimal cutoffs (Figs. 6A and 6B; Table 3).

DISCUSSION

In this study, we demonstrated 2 different quantitative methods, Δ TBS and Δ nPC, as effective means for early prediction of [¹⁷⁷Lu]Lu-DOTATATE treatment response. The capability to distinguish PD from non-PD groups became apparent as early as the second posttreatment scan; Δ nPC_{second-first} showed an AUC of 0.764, sensitivity of 71.4%, and specificity of 75%, whereas Δ TBS_{second-first} showed an AUC of 0.793, sensitivity of 71.4%, and specificity of 85%. These results indicate the possibility of identifying—as early as 2 mo after the treatment initiation—patients who will not respond.

The early identification of treatment response, particularly a lack of response, holds significant importance. First, it can facilitate timely transitions to alternative treatment options, potentially optimizing patient outcomes. Also, [¹⁷⁷Lu]Lu-DOTATATE is known to be associated with several side effects. Long-term side effects include hepatotoxicity, nephrotoxicity, and myelotoxicity, with deterioration in all cell lines, persisting up to a year after therapy (15–18). Late organ injuries and secondary neoplasms have also been reported (19). Notably, in the final reports of the NETTER-1 trial, 2% of patients treated with [¹⁷⁷Lu]Lu-DOTATATE developed myelodysplastic syndrome, with one case resulting in a treatment-related death (5). Moreover, the high cost of this treatment, averaging \$50,000 per dose in the United States and even more when including labor and other expenses, poses a substantial financial burden (20). Although studies in Europe have deemed this treatment

TABLE 3
ROC Results for Δ TBS and Δ nPC

Parameter	AUC	95% CI	Cutoff	Sensitivity (%)	Specificity (%)	Youden index
Δ TBS _{second-first}	0.793	0.596–0.99	0.039	71.4	85	0.564
Δ TBS _{third-first}	0.893	0.753–1.033	0.040	71.4	95	0.664
Δ TBS _{fourth-first}	0.957	0.885–1.03	0.077	100	80	0.8
Δ nPC _{second-first}	0.764	0.546–0.983	-0.176	71.4	75	0.464
Δ nPC _{third-first}	0.693	0.477–0.908	-0.119	71.4	70	0.414
Δ nPC _{fourth-first}	0.679	0.448–0.909	-0.513	100	35	0.350

ROC = receiver operating characteristic.

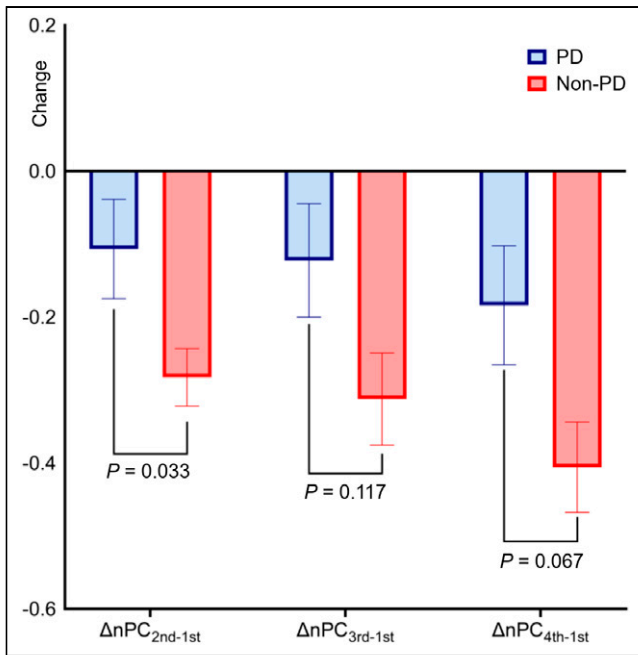


FIGURE 5. Mean ΔnPC comparison of PD and non-PD throughout treatment sessions. Lines represent SE of mean. P values were calculated using independent-samples t test.

cost-effective, such analysis is lacking in the United States (21,22). Redirecting to alternative therapies patients who are unlikely to respond could potentially enhance cost-effectiveness, a critical consideration in health care decision-making.

It has been suggested that tumor load should be considered before treatment initiation (23,24), as patients with low-volume tumors may respond more favorably to ^{177}Lu than patients with bulky disease, and in cases of bulky disease, other radionuclides such as ^{90}Y could be considered, given that the β -emission of ^{90}Y has an increased mean tissue range compared with ^{177}Lu (25). However, in our study the mean TBS in the non-PD group was higher than in the PD group at treatment initiation. But in the non-PD group, TBS exhibited a sudden decrease on therapy initiation, whereas in the PD group TBS continued to rise. This suggests that initial tumor burden should not be the sole indicator of treatment response or selection of treatment modality; rather, the change should be considered. The inter- and intratumoral heterogeneity of GEP-NETs might underlie this phenomenon (26). The fact that

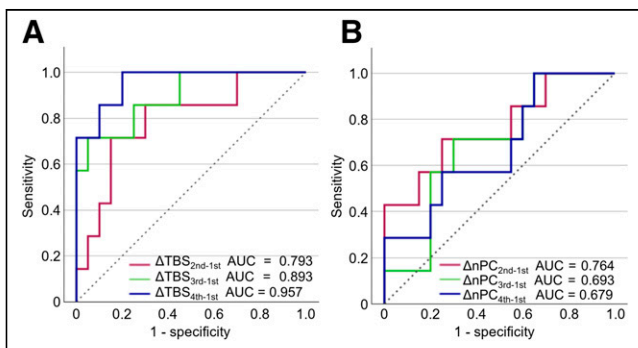


FIGURE 6. Receiver operating characteristic curves for ΔTBS (A) and ΔnPC (B).

these tumors, especially the pancreatic ones, often comprise multiple cell types (27,28) could lead to variations in their susceptibility to treatment. Moreover, it was shown that patients with heterogeneous somatostatin receptors on target lesions had significantly worse outcomes than did patient with homogeneous expression (29). Our findings regarding ΔnPC may support this hypothesis. Even mean nPC values were higher in the non-PD group than in the PD group. The mean nPC values began to decline rapidly after the first treatment session, contrary to the PD group, which remained relatively stable. However, this decline slowed through the last scan—a finding that is possibly attributable to the death of treatment-susceptible cell lines throughout the treatment timeline. Another explanation could be the fact that lower-grade tumors typically exhibit a higher concentration of somatostatin 2 receptors (30), potentially leading to a higher initial nPC . This could signify a dramatic ΔnPC since lower-grade tumors are more susceptible to treatment. Moreover, lesions with higher nPC s might receive a greater radiation dose due to their higher receptor count. It is arguable that PD patients might have received a subtherapeutic dose for the same reason. Ha et al. (31) calculated tumor-absorbed dose estimated from ^{177}Lu Lu-DOTATATE SPECT/CT and found a statistical association between a higher cumulative dose and disease control in the target lesion. Similar to our findings, they did not find an association between response and first-cycle SUV_{peak} . On the contrary, Alipour et al. (32) found that first-cycle radiation dose in measurable lesions was associated with local response but not survival. Studies using ^{68}Ga -DOTATATE PET revealed similar results. Mileva et al. (33) found that patients with a somatostatin receptor tumor volume decrease of more than 10% after the first session, as well as a minimal first-cycle dose of 35 Gy in all target lesions, exhibited significantly longer progression-free survival. Our findings support the importance of incorporating postcycle imaging into standard peptide receptor radionuclide therapy workflows, as described by Yadav et al. (34). We believe our analysis is practical and convenient for clinical settings, in view of the straightforward mathematic formulations that can easily be automated and accommodate high clinical volumes. As the importance of artificial intelligence in radiology grows, methodologies such as ours, showing clinical promise, are valuable for developers aiming to enhance traditional practices.

One intriguing finding is that 5 of 7 PD patients reported clinical improvement at the third-month follow-up. We investigated whether pseudoprogression could be responsible for this. However, chart reviews revealed that 3 of them had sixth-month follow-up CT available and that this follow-up CT also showed PD. Among the patients with unavailable CT, one died at the ninth month because of disease-related complications, making pseudoprogression less likely. All non-PD patients reported better clinical outcomes at the third month.

Our study bears limitations because of its small sample size, particularly within the PD group. Prospective studies are imperative to substantiate and validate our findings.

CONCLUSION

ΔTBS and ΔnPC can predict ^{177}Lu Lu-DOTATATE response by the second treatment session.

DISCLOSURE

No potential conflict of interest relevant to this article was reported.

KEY POINTS

QUESTION: Can response to [¹⁷⁷Lu]Lu-DOTATATE treatment be predicted earlier in the treatment course?

PERTINENT FINDINGS: In this retrospective study, Δ TBS and Δ nPC were able to distinguish response groups as early as the second posttreatment scan. Δ nPC_{second-first} showed a sensitivity of 71.4% and a specificity of 75%, whereas Δ TBS_{second-first} showed a sensitivity of 71.4% and a specificity of 85%. Δ TBS_{fourth-first} exhibited an AUC of 0.957, achieving 100% sensitivity and 80% specificity.

IMPLICATIONS FOR PATIENT CARE: Δ TBS and Δ nPC can predict response to [¹⁷⁷Lu]Lu-DOTATATE by the second session, enabling early switching to other therapeutic options to prevent wasting of time and resources and to minimize toxicities.

REFERENCES

- Hennrich U, Kopka K. Lutathera®: the first FDA- and EMA-approved radiopharmaceutical for peptide receptor radionuclide therapy. *Pharmaceuticals (Basel)*. 2019;12:114.
- Dash A, Chakraborty S, Pillai MR, Knapp FF Jr. Peptide receptor radionuclide therapy: an overview. *Cancer Biother Radiopharm*. 2015;30:47–71.
- Mejia A, Vivian E, Nwogu C, et al. Peptide receptor radionuclide therapy implementation and results in a predominantly gastrointestinal neuroendocrine tumor population: a two-year experience in a nonuniversity setting. *Medicine (Baltimore)*. 2022;101:e28970.
- Strosberg J, El-Haddad G, Wolin E, et al. Phase 3 trial of ¹⁷⁷Lu-Dotatate for midgut neuroendocrine tumors. *N Engl J Med*. 2017;376:125–135.
- Strosberg JR, Caplin ME, Kunz PL, et al. ¹⁷⁷Lu-Dotatate plus long-acting octreotide versus high-dose long-acting octreotide in patients with midgut neuroendocrine tumours (NETTER-1): final overall survival and long-term safety results from an open-label, randomised, controlled, phase 3 trial. *Lancet Oncol*. 2021;22:1752–1763.
- Simron Singh et al. [¹⁷⁷Lu]Lu-DOTA-TATE in newly diagnosed patients with advanced grade 2 and grade 3, well-differentiated gastroenteropancreatic neuroendocrine tumors: primary analysis of the phase 3 randomized NETTER-2 study. *J Clin Oncol*. 2024;42:LBA588.
- Herrmann K, Schwaiger M, Lewis JS, et al. Radiotheranostics: a roadmap for future development. *Lancet Oncol*. 2020;21:e146–e156.
- Application number: 208700Orig1s000—product quality review(s). U.S. FDA website. https://www.accessdata.fda.gov/drugsatfda_docs/nda/2018/208700Orig1s000ChemR.pdf. Published December 23, 2017. Accessed August 19, 2024.
- Eisenhauer EA, Therasse P, Bogaerts J, et al. New response evaluation criteria in solid tumours: revised RECIST guideline (version 1.1). *Eur J Cancer*. 2009;45:228–247.
- syngo.via: get the full picture. Siemens Healthineers website. <https://www.siemens-healthineers.com/en-us/molecular-imaging/pet-ct/syngo-via>. Accessed August 19, 2024.
- Sasaki K, Morioka D, Conci S, et al. The tumor burden score: a new “metro-ticket” prognostic tool for colorectal liver metastases based on tumor size and number of tumors. *Ann Surg*. 2018;267:132–141.
- Sasaki K, Margonis GA, Andreatos N, et al. The prognostic utility of the “tumor burden score” based on preoperative radiographic features of colorectal liver metastases. *J Surg Oncol*. 2017;116:515–523.
- Deng G, Ren JK, Wang HT, et al. Tumor burden score dictates prognosis of patients with combined hepatocellular cholangiocarcinoma undergoing hepatectomy. *Front Oncol*. 2023;12:977111.
- Ho SY, Liu PH, Hsu CY, et al. Tumor burden score as a new prognostic marker for patients with hepatocellular carcinoma undergoing transarterial chemoembolization. *J Gastroenterol Hepatol*. 2021;36:3196–3203.
- Bergsma H, Konijnenberg MW, van der Zwan WA. Nephrotoxicity after PRRT with ¹⁷⁷Lu-DOTA-octreotate. *Eur J Nucl Med Mol Imaging*. 2016;43:1802–1811.
- Sabet A, Ezziddin K, Pape UF. Accurate assessment of long-term nephrotoxicity after peptide receptor radionuclide therapy with ¹⁷⁷Lu-octreotate. *Eur J Nucl Med Mol Imaging*. 2014;41:505–510.
- Saracyn M, Durma AD, Bober B, et al. Long-term complications of radioligand therapy with lutetium-177 and yttrium-90 in patients with neuroendocrine neoplasms. *Nutrients*. 2022;15:185.
- Bergsma H, van Lom K, Raaijmakers MHGP. Persistent hematologic dysfunction after peptide receptor radionuclide therapy with ¹⁷⁷Lu-DOTATATE: incidence, course, and predicting factors in patients with gastroenteropancreatic neuroendocrine tumors. *J Nucl Med*. 2018;59:452–458.
- Salner AL, Blankenship B, Dunnack H, Niemann C, Bertsch H. Lutetium Lu-177 dotatate flare reaction. *Adv Radiat Oncol*. 2020;6:100623.
- Suisson G, Huang R. The implementation of Lutathera® therapy [abstract]. *J Nucl Med*. 2022;63(suppl. 2):4074.
- Smith-Palmer J, Leeuwenkamp OR, Virk J, Reed N. Lutetium oxodotretotide (¹⁷⁷Lu-Dotatate) for the treatment of unresectable or metastatic progressive gastroenteropancreatic neuroendocrine tumors: a cost-effectiveness analysis for Scotland. *BMC Cancer*. 2021;21:10.
- Hagendijk ME, van der Schans S, Boersma C, Postma MJ, van der Pol S. Economic evaluation of orphan drug lutetium-octreotate vs. octreotide long-acting release for patients with an advanced midgut neuroendocrine tumour in the Netherlands. *Eur J Health Econ*. 2021;22:991–999.
- Virgolini I. Overall survival results from the NETTER-1 trial in neuroendocrine tumours: an important milestone. *Lancet Oncol*. 2021;22:1645–1646.
- Paganelli G, Sansovini M, Ambrosetti A, et al. ¹⁷⁷Lu-Dota-octreotate radionuclide therapy of advanced gastrointestinal neuroendocrine tumors: results from a phase II study. *Eur J Nucl Med Mol Imaging*. 2014;41:1845–1851.
- Uccelli L, Boschi A, Cittanti C, et al. ⁹⁰Y/¹⁷⁷Lu-DOTATOC: from preclinical studies to application in humans. *Pharmaceutics*. 2021;13:1463.
- Hoffman SE, Dowrey TW, Villacorta Martin C, et al. Intertumoral lineage diversity and immunosuppressive transcriptional programs in well-differentiated gastroenteropancreatic neuroendocrine tumors. *Sci Adv*. 2023;9:eadd9668.
- Hofving T, Arvidsson Y, Almobarak B, et al. The neuroendocrine phenotype, genomic profile and therapeutic sensitivity of GEPNET cell lines. *Endocr Relat Cancer*. 2018;25:367–380.
- Viol F, Sipos B, Fahl M, et al. Novel preclinical gastroenteropancreatic neuroendocrine neoplasia models demonstrate the feasibility of mutation-based targeted therapy. *Cell Oncol (Dordr)*. 2022;45:1401–1419.
- Graf J, Pape UF, Jann H, et al. Prognostic significance of somatostatin receptor heterogeneity in progressive neuroendocrine tumor treated with Lu-177 DOTATOC or Lu-177 DOTATATE. *Eur J Nucl Med Mol Imaging*. 2020;47:881–894.
- Fabritius MP, Soltani V, Cyran CC, et al. Diagnostic accuracy of SSR-PET/CT compared to histopathology in the identification of liver metastases from well-differentiated neuroendocrine tumors. *Cancer Imaging*. 2023;23:92.
- Ha S, Kim Y, Oh JS, Yoo C, Ryoo BY, Ryu JS. Prediction of [¹⁷⁷Lu]Lu-DOTA-TATE therapy response using the absorbed dose estimated from [¹⁷⁷Lu]Lu-DOTA-TATE SPECT/CT in patients with metastatic neuroendocrine tumour. *EJNMMI Phys*. 2024;11:14.
- Alipour R, Jackson P, Bressel M, et al. The relationship between tumour dosimetry, response, and overall survival in patients with unresectable neuroendocrine neoplasms (NEN) treated with ¹⁷⁷Lu DOTATATE (LuTate). *Eur J Nucl Med Mol Imaging*. 2023;50:2997–3010.
- Mileva M, Marin G, Levillain H, et al. Prediction of ¹⁷⁷Lu-DOTATATE PRRT outcome using multimodality imaging in patients with gastroenteropancreatic neuroendocrine tumors: results from a prospective phase II LUMEN study. *J Nucl Med*. 2024;65:236–244.
- Yadav S, Lawhn-Heath C, Paciorek A, et al. The impact of posttreatment imaging in peptide receptor radionuclide therapy. *J Nucl Med*. 2024;65:409–415.